Electronic and Magnetic Properties of Activated Carbon Fibers

Atsuko Nakayama,* Kazuya Suzuki, Toshiaki Enoki, Kei-ichi Koga,† Morinobu Endo,†† and Norifumi Shindo†††

Department of Chemistry, Tokyo Institute of Technology, Ookayama, Meguro-ku, Tokyo 152

†Institute for Solid State Physics, The University of Tokyo, Roppongi, Minato-ku, Tokyo 106

††Department of Electrical Engineering, Faculty of Engineering, Shinsyuu University, Wakazato, Nagano 380

†††Osaka Gas Corporation, Torishima, Konohana-ku, Osaka 554

(Received July 24, 1995)

Activated carbon fibers (ACF) consist of microporous carbon with a huge specific surface area (SSA) ranging from 700 $m^2 g^{-1}$ to 3000 $m^2 g^{-1}$, and a having random structures consisting of an assembly of micrographites with a dimension of ca. 20×20 Å^2. The electrical conductivity and magnetic susceptibility were investigated for ACFs with SSA = 1000 and 2000 $m^2 g^{-1}$ in order to clarify the relation between the electronic properties and the structure of ACF having a random network of micrographites. The electrical conductivity is explained by the two-dimensional variable-range hopping conduction at lower temperatures and thermally activated conduction at higher temperatures. The introduction of N_2 or O_2 gas to a sample induces a change in the conductivity, which is considered to be caused by a structural change and a charge transfer between dangling bonds and O_2 gas. The observed value of the orbital diamagnetic susceptibility is considerably small compared with that of a condensed polycyclic aromatic hydrocarbon having the same dimensions as that of the micrographite in ACF. This implies that the micrographitic domains have a deformed planar structure with the presence of defects.

Activated carbon fibers (ACF) are a kind of microporous carbon having enormous specific surface areas (SSA), ranging from 700 to 3000 $m^2 g^{-1}$. The manufacturing process, called "activation", gives a porous structure to the fibers, resulting in making the SSA larger than other porous materials. Therefore, ACF is well known as an absorbent; there have been several reports concerning its gas adsorption properties.[1)]

From the point of solid state properties, various studies have recently been carried out in order to obtain information concerning the structures, electronic properties, and magnetism. The X-ray diffraction,[2)] Raman spectra,[3)] transmission electron-microscope observations,[4)] and gas adsorption[1)] were analyzed in order to clarify the porous ACF structure. According to a structure model proposed by Kaneko et al.,[5)] ACF consists of an assembly of many micrographites which form disordered stacks of three to four graphene sheets with dimensions of ca. 20×20 Å^2. An assembly of many micrographites forms a network structure, resulting in the presence of micropores with a dimension of 10 to 20 Å. There are dangling bonds and functional groups at the peripheries of the micropores, which produce localized spins. The presence of these micropores is the origin of the enormous specific surface areas, which can accept a huge amount of gaseous materials.

The transport properties provide information about the electronic structure related to the network of micrographitic domains. The resistivity, the magnitude of which at room temperature is 2×10^{-3} Ω m[7)] is on the same order as that for phenol-based carbon fibers,[6)] and is explained in terms of the two-dimensional variable-range hopping (2D VRH) related to a disordered structural network of metallic micro-graphitic domains. The same trend was observed regarding magnetoresistance having a weakly positive value at low temperatures.[7)] A heat-treatment of ACFs at high temperatures of 1300—2800 °C reduces the magnitude of the randomness in the structure, and induces a strong modification of the electronic structure,[8)] which can be explained by "the σ-trap mechanism" proposed by Morozowski.[9)] The functional groups are removed from the marginal regions of the micrographites upon heat-treating the samples, resulting in the generation of σ-type dangling bonds. In this process, conduction π-electrons are trapped by unsaturated σ-bondings, and, consequently, the same number of holes are generated in the valence π-band. Thus, the number of carriers at the Fermi level changes upon a heat-treatment, and the magnitude of the mean free path of the carriers increases along with an enlargement of the size of the crystallites above heat-treatment temperatures of 2800 °C.

Meanwhile, concerning magnetism, the porous structure of ACF has many defects and dangling bond spins. In this respect, ESR and the magnetic susceptibility measurements are helpful for understanding the micro structure at the peripheries of micrographite. Especially, the combination of ESR and gas adsorption measurements provides information about the interaction between the introduced gaseous

molecule and the dangling bond spin, as well as the structural modification of the micropores generated by gas uptake.[10] An investigation of the dangling bond spin ESR signal under an oxygen atmosphere has revealed the formation of weak bounding between the oxygen molecules and the dangling bond spin in the micropores.

As mentioned above, recent studies have been devoted to understanding the solid state properties of ACFs related to the disordered microporous network structure. However, there is little information about the structure of the micrographitic domain, itself. In addition, the effect of gas adsorption on the solid state properties has not been well understood. In this study, the electrical conductivity and magnetic susceptibility were investigated for pitch-based ACF1000 and 2000 having SSA = 1000 and 2000 $m^2 g^{-1}$ in order to clarify the structure and electronic properties of micrographitic domains with random structures. Moreover, the gas adsorption effects on the electrical conductivities were investigated in order to find the relationship between the gas adsorption state and a change in the conductivity.

Experimental

Sample Preparation and Characterization. In the present experiments, we employed pitch-based ACF with SSA = 1000 and 2000 $m^2 g^{-1}$ (ACF1000 and ACF2000) produced by Osaka Gas Corporation. ACF pristine samples were made from spun fibers after the precursors which had started from petroleum pitch underwent an antiflammable process at 300 °C in air. During the activation process, the fibers were carbonized at 800 to 1200 °C in the presence of either CO_2 or water vapor. In this process, a highly porous structure of ACF was made by depriving carbon atoms from the precursors through the oxidation reaction. The magnitude of SSA was measured by the adsorption isotherms of N_2 at 77 K and CO_2 at 195 K.

Electrical Conductivity. The electrical conductivities for ACF1000 and ACF2000 were measured by the direct current four-probe method from 30 to 285 K. Four electrical contacts were achieved by sandwiching an ACF fiber between four grafoil pieces and a quartz plate having four electrodes of evaporated gold films. In order to determine the absolute value of the electrical conductivity (σ), scanning electron microscopy (SEM) was used to measure the fiber diameters. The gas adsorption effects for the electrical conductivities were investigated for oxygen gas and nitrogen gas which had been introduced into a sample of ACF1000. A specially designed cell (shown in Fig. 1) was used to measure the electrical conductivity in an atmosphere of nitrogen gas or oxygen gas. The sample was heated at 200 °C and ca. 10^{-5} Torr before introducing gas into the cell (1 Torr = 133.322 Pa). Then, 700 Torr nitrogen gas or oxygen gas was introduced at room temperature.

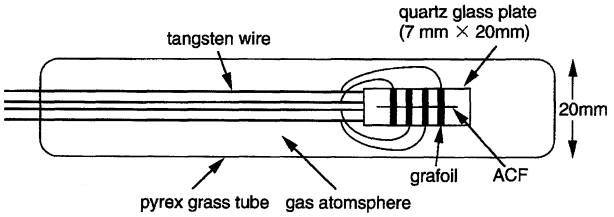

Fig. 1. The glass cell for the measurement of electrical conductivities for the gas adsorbing sample.

Magnetic Susceptibility. The magnetic susceptibilities were measured over the temperature range from 4 to 300 K using an automatic magnetic pendulum in an applied field of $H = 1$ T.

Results

The temperature dependences of the electrical conductivities (σ) are shown in Fig. 2 (a) for ACF1000 and ACF2000 over the entire observed temperature range. The temperature dependences of the conductivities show a semiconductive behavior with similar characteristics as those of ACF1000 and ACF2000. Discontinuous changes in plots observed above ca. 150 K are associated with changes in the contact resistance at the interface between the sample and the electrodes, which were generated by thermal contraction. The absolute values of the conductivities of both ACF1000 and ACF2000 at room temperature were estimated to be 4.5 and 7.5 S cm^{-1}, respectively, by using the fiber diameters obtained from the SEM results, as shown in the photograph of Fig. 3. The fiber diameters were estimated to be 18 μm for both the ACF1000 and ACF2000 samples. SEM photographs show that the cross sections of the fibers are rather regular rounds having a smooth surface.

Figure 2 (b) shows plots of $\ln(\sigma/\sigma_{r.t.})$ vs. $T^{-1/3}$ below ca. 80 K for ACF1000 and ACF2000. According to the result shown in Fig. 2 (b), the conductivity obeys an $\exp((-\frac{T_0}{T})^{\frac{1}{3}})$ dependence at low temperature, below 80 K, where the T_0s are estimated to be 2.0×10^4 K for both ACF1000 and ACF2000. Figure 2 (c) shows a $\ln\sigma$ vs. $1/T$ plot above 180 K, which suggests that the conductivity is dominated by a thermal activation process, $\exp(-\Delta E/kT)$, in the higher temperature range. From the results shown in Fig. 2 (c), ΔE was estimated to be 60 to 80 meV on the average for 3 samples for both ACF1000 and ACF2000, which is in semi-quantitative agreement with the activation energy ($\Delta E \approx 44$ meV) obtained by an ESR measurement of ACF3000 having SSA = 3000 $m^2 g^{-1}$.[11] An analysis of the temperature dependence of the conductivities is carried out in relation to the electronic state in "Discussion".

In order to investigate the influence of gas adsorption on the transport property of ACF, the time dependence of the resistivities of ACF1000 was measured under an oxygen gas or a nitrogen gas atmosphere at room temperature. In Fig. 4, the time dependences of the variation rates of the resistivities are plotted before and after introducing of 700 Torr nitrogen or oxygen gas at room temperature. The introduction of nitrogen gas makes the resistivity increase by less than 1% in 200 min. The increase is saturated within about 50 min. Meanwhile, for oxygen gas, a steep resistivity increase has been observed in the first 10 min, and the total resistivity increase reaches ca. 3.5% for 200 min. Details concerning the adsorption states of these gases are mentioned in "Discussion".

The temperature dependence of the magnetic susceptibilities of ACF1000 and ACF2000 are shown in Fig. 5. The susceptibilities for both ACF1000 and ACF2000 show a diamagnetic behavior at high temperatures above about 20—30 K, while they obey the Curie–Weiss law at low temperatures,

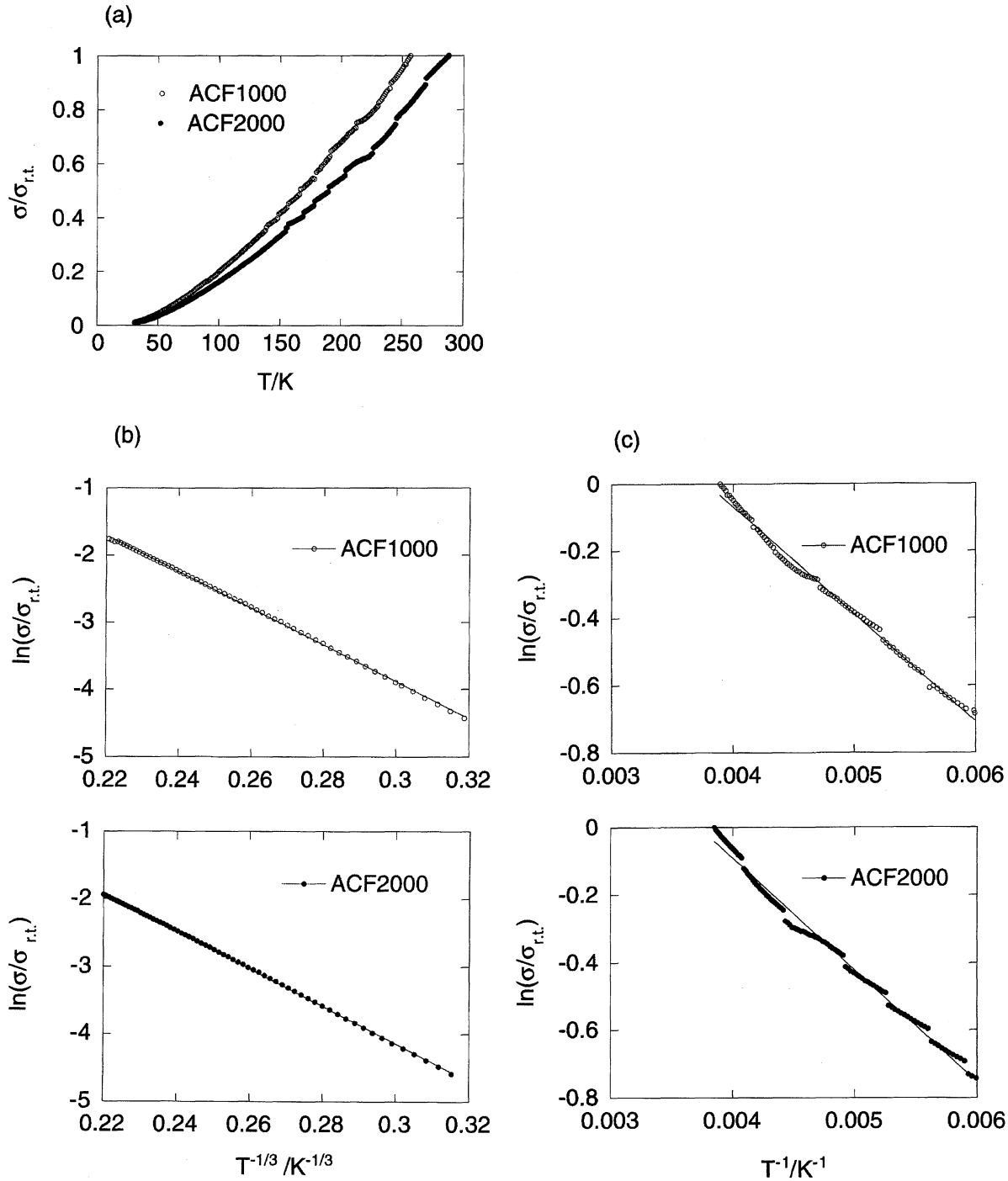

Fig. 2. The temperature dependence of the conductivity σ for ACF1000 and ACF2000 from 30 K to room temperature; (a) plots of σ vs. T, (b) plots of $\ln(\sigma/\sigma_{r.t.})$ vs. $T^{-1/3}$ in the low temperature range below about 80 K, (c) plots of $\ln(\sigma/\sigma_{r.t.})$ vs. T^{-1} in the high temperature range above about 180 K. Discontinuous changes in the plots obtained above ca. 150 K are associated with the changes in contact resistance at the interface between the sample and the electrodes which were generated by thermal contraction.

as does ACF3000.[10] The observed magnetic susceptibility of ACF (χ_{obs}) consists of the following components:

$$\chi_{obs} = \chi_C + \chi_{Pauli} + \chi_{orb} + \chi_{core}, \quad (1)$$

where χ_C is the Curie–Weiss component of localized spins, χ_{Pauli} the Pauli paramagnetic component for conduction electrons, χ_{orb} the orbital diamagnetic component, and χ_{core} the Pascal diamagnetic component. The observed magnetic susceptibility (χ_{obs}) below 40 K gives a Curie–Weiss component (χ_C) having localized spin concentrations of $N_C=2.2\times10^{19}$ g^{-1} and $N_C=3.3\times10^{19}$ g^{-1} in the antiferromagnetic molecular field of Weiss temperatures of $\theta=-0.6$ K and $\theta=-1.3$ K for ACF1000 and ACF2000, respectively, as summarized in Table 1. The component of χ_C is thought to be caused by the dangling bond spins being at the peripheries of the mi-

Table 1. Contributions of Curie–Weiss spin-paramagnetism χ_C, Pauli-paramagnetism χ_{Pauli}, orbital diamagnetism $\chi_{//orb}$ and core diamagnetism χ_{core} to the observed magnetic susceptibility χ_{obs} measured at room temperature, where $\chi_{//orb}$ is the orbital susceptibility in the field perpendicular to the graphitic plane. N_C and θ are the localized spin concentration and the Weiss temperature, respectively, in the Curie–Weiss susceptibility.

Sample	χ_{obs}/emu g^{-1}	χ_C/emu g^{-1}	θ/K	N_C	$\chi_{//orb}$/emu g^{-1}	χ_{core}/emu g^{-1}	χ_{Pauli}/emu g^{-1}
ACF1000	-7.9×10^{-7}	4.9×10^{-8}	−0.6	2.2×10^{19}	-1.2×10^{-6}	-5.6×10^{-7}	1.1×10^{-7}
ACF2000	-7.3×10^{-7}	6.8×10^{-8}	−1.3	3.3×10^{19}	-1.1×10^{-6}	-5.6×10^{-7}	1.1×10^{-7}

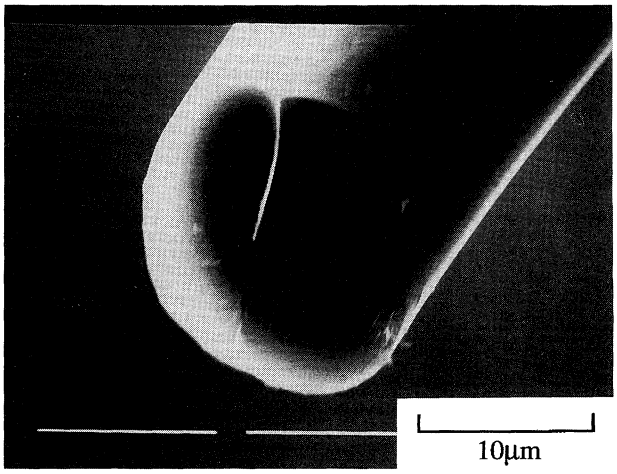

Fig. 3. Scanning electron microscopy (SEM) photograph of the cross section of pitch based ACF1000 (m^2 g^{-1}).

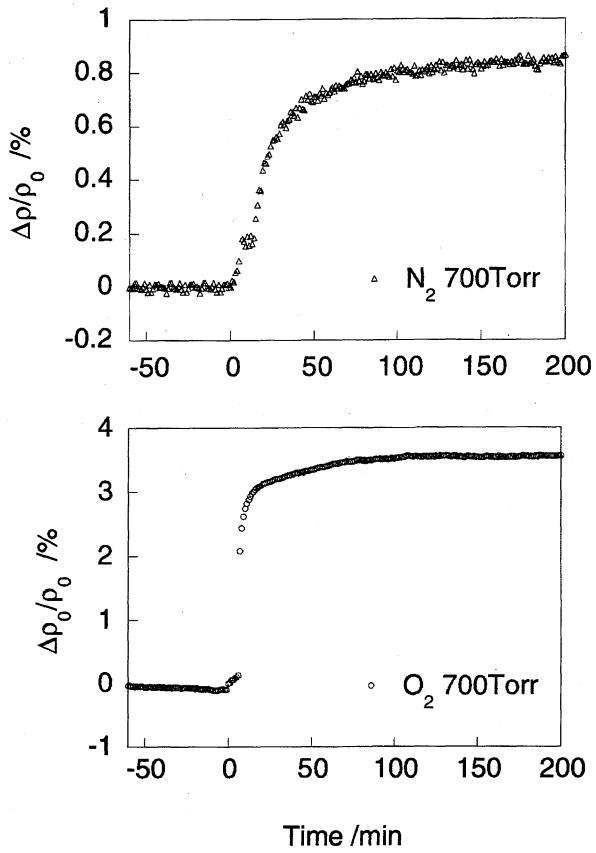

Fig. 4. Time dependence of the variation rate of the resistivity for ACF1000 adsorbing 700 Torr N_2 gas (△) and 700 Torr O_2 gas (○) at room temperature. The vertical axis represents the percentage of the variation rate of the resistivity ρ. ρ_0 is the value of the resistivity at the zero point of the time which shows the starting point of the gas adsorption.

crographitic domains. The obtained spin concentrations are about the same as the spin concentration of ACF3000.[10] This suggests that the dangling bond spin concentration does not depend on the value of SSA among the ACF1000, ACF2000, and ACF3000 samples. The core contributions (χ_{core}) were estimated at $\chi_{core}=-5.6\times10^{-7}$ emu g^{-1} for both ACF1000 and ACF2000 on the basis of the composition ($[C_{124}H_{80}NO]_n$[12]) using Pascal's rule. For an analysis of the Pascal diamagnetism, we assume the mean structure of ACF, which is described in terms of the aromatic part having 36 benzene rings and the remaining aliphatic bridging part, taking into account the composition and micrographitic domain size of ACF. The contributions of χ_{Pauli} and χ_{orb} are estimated in the next section (summarized in Table 1).

Discussion

We extracted information concerning the electronic structure of ACF from an analysis of the conductivity. The density of states (DOS) at the Fermi level $N(E_F)$ in the case of 2D VRH was estimated to be as follows. Judging from the random structure of ACF composing an Assembly of micrographites, it is supposed that the electrons are localized on metallic micrographites, and that hopping conduction occurs between micrographites due to a thermal activation process. Around the marginal region of the micrographites, the wave functions of the electrons attenuate in accordance with the function of $\exp(-r/\xi)$, where ξ is the localization length, so that the overlap between the wave functions of the adjacent micrographitic domains is in proportion to $\exp(-2r/\xi)$. Moreover, the occurrence of a hopping event requires thermal activation, which is related to the difference in the potential energies of the hopping electrons (ΔE). Thus, the hopping conductivity (σ) is expressed by

$$\sigma = \sigma_0 \exp\left(-2\alpha r - \frac{\Delta E}{kT}\right), \tag{2}$$

where σ_0 is a constant.[13] ΔE depends on DOS at the Fermi energy level ($N(E_F)$) and the dimensionality of the transport system of ACF. In a random network system of metallic microdomains having two-dimensionality, the conductivity expressed in Eq. 2 can be rewritten using the variable-range hopping formula at various temperatures as;

$$\sigma = \sigma_0 \exp\left(\left(-\frac{T_0}{T}\right)^{\frac{1}{3}}\right). \tag{3}$$

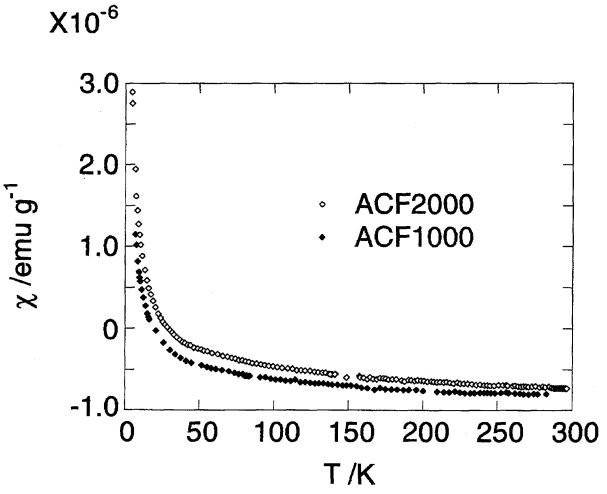

Fig. 5. Temperature dependence of magnetic susceptibility for ACF1000 (◆) and ACF2000 (◇).

Here, T_0 is expressed by

$$T_0 = \frac{27}{\xi^2 \pi N(E_F) k}, \quad (4)$$

where k is the Boltzmann constant. As shown in the previous section, the temperature dependence observed below 50 K can be explained in terms of the two-dimensional variable-range hopping (2D VRH),[13] taking into account the two-dimensionality of the micrographite network structure of ACF. The in-plane size of a micrographite (L_a) in ACF was estimated to be $L_a \approx 25$ Å from the Raman spectra.[1,3] The range where electrons can move coherently on ACF is limited to within a micrographite domain which is regarded as a metallic island, and the conduction electrons are scattered at the boundaries of the micrographites. Therefore, if we assume ξ to be the in-plane size of a micrographite ($\xi \approx 25$ Å), DOS is estimated to be $N(E_F)=8\times10^{17}$ eV^{-1} m^{-2} for both ACF1000 and ACF2000. This suggests that ACF1000 and ACF2000 have almost similar electronic structures, taking into account the similar behavior of the magnetic susceptibilities for both samples, which are mentioned later.

We now discuss the relation between the micrographite network structure and the two-dimensionality in the electron transport observed in the present experiment. In general, there are two kinds of micrographitic carbons: One is a graphitizing carbon with a two-dimensional orientation of micrographites; the other is a nongraphitizing carbon with a random orientation of micrographites, as proposed by Frankline.[14] In the case of ACF, according to the X-ray diffraction analyses[1] and Raman spectra,[2] it is found that ACF consists of an assembly of 2D-micrographites. The result of a diamagnetic susceptibility suggests that an ACF sample heat-treated at 1500 to 3000 °C is well graphitized,[5] with two-dimensionally preferred orientations of micrographites. Judging from the structural information, ACF is classified to be in the former category, and it is supposed that the micrographites are linked to each other by σ-bondings extending in the two-dimensional directions, and that the micrographite network has a disordered structure showing the two-dimensionality to some extent. It is therefore reasonable that the VRH mechanism observed below 50 K can be explained based on the two-dimensionality of the micrographite network structure. Also, the electrons hop between micrographites in two-dimensional directions through the σ-bonding bridges, which cause an overlapping of the wave functions between adjacent micrographites.

We now discuss the relationship between the gas adsorption and conduction mechanism for ACF. Non-active nitrogen gas is known to induce a structural change in the micrographite of ACF.[15] According to nitrogen gas adsorption at 165 K, the interlayer distance between graphitic sheets decreases by 6% upon introducing nitrogen gas, even though the amount is less than 5% of the saturated amount.[15] The change in the interlayer distance of the micrographite is explained by the relation between the structure of ACF and the adsorption site of the nitrogen molecules. Since the micropore of ACF is characterized by a wedge-type pore, nitrogen molecules can easily enter into the wedge-type pore through a wide-open entrance at the side surface of the micrographite. The adsorption of nitrogen gas changes the micropore shape from the wedge type to the slit type, which causes a slight expansion of the ACF network structure. The conductive pass connecting the micrographites existing before nitrogen gas adsorption is cut by a reorientation of the micrographites after nitrogen gas adsorption. Therefore, a change in the stacking structure affects the network structure between the micrographites, and, as a result, causes an increase in the resistivity by nitrogen uptake. In the case of the adsorption of oxygen gas, the adsorption site is supposed to be different from that of the nitrogen gas. Based on the ESR spectra assigned to the dangling bond spins existing at the peripheries of micrographites,[10] the change of the ESR signal due to introducing the oxygen gas suggests the formation of weak covalent bonds between the dangling bonds and oxygen molecules. Namely, in the case of oxygen gas adsorption, the ESR saturation curve behaves as a homogeneous spin system, which is different from the behavior of the curves in nitrogen gas, show trends for an inhomogeneous spin system.[16] In addition, the adsorption isotherm for oxygen at room temperature has a different behavior from that for inert gases, inducing nitrogen gas, which reveals evidence for the formation of weak chemical bondings. The adsorption of water vapor is informative for explaning oxygen gas adsorption to ACF,[15] since the adsorption manner of water molecules is supposed to be similar to that of oxygen molecules, based on the trend of chemical activity. Water molecules are gradually introduced into the parts in which the functional groups are located, and no structural change of the micrographite is induced until water molecules are adsorbed in the interlayer space of the micrographite changing the orientation of micrographites. Therefore, the steep change in the resistivity at the beginning of the adsorption is considered to be associated with the formation of weak covalent bonds with oxygen, which induces not only charge transfer between the oxygen molecules and micrographite,

but also a structural change.

Finally, we consider the electronic structure based on the results of the magnetic susceptibilities and the conductivities, and attempt to obtain information concerning the geometrical structure of the micrographite, itself. The values of χ_{Pauli} for both ACF1000 and ACF2000 were calculated to be 1.1×10^{-7} emu g^{-1} from $\chi_{\text{Pauli}}=2\mu_B^2N(E_F)$ by using $N(E_F)$, whose values were obtained from the variable-prange hopping conductivity. After subtracting the values of χ_C, χ_{Pauli}, and χ_{core} from the observed susceptibility (χ_{obs}), we obtained the contributions of χ_{orb} for samples having randomly oriented micrographite planes: -3.9×10^{-7} emu g^{-1} for ACF1000 and -3.5×10^{-7} emu g^{-1} for ACF2000. The value of the orbital susceptibility ($\chi_{\text{orb}//}$) in the field applied perpendicular to the graphitic plane was obtained to be -1.2×10^{-6} and -1.1×10^{-6} emu g^{-1} for ACF1000 and ACF2000, respectively, by multiplying by 3, since the graphitic microdomains are randomly oriented. The observed absolute values of $\chi_{//\text{orb}}$ for ACF1000 and ACF2000 are one order of magnitude smaller than the value ($\chi_{//\text{orb}}=-8\times10^{-6}$ emu g^{-1}) for graphite, having an infinitely extended planar structure of condensed polycyclic aromatic hydrocarbon.[17] The component $\chi_{//\text{orb}}$ for graphite originates from delocalized π-electrons on an infinite graphitic plane. Therefore, the fact that ACF has a smaller orbital diamagnetism than graphite proves that the micrographitic domain in ACF has a finite size. Then, the magnitude of $\chi_{//\text{orb}}$ of ACF is compared with other condensed polycyclic aromatic hydrocarbons having finites size and graphite fine particles. The magnitude of the orbital diamagnetic susceptibility for graphite fine particles having a domain size of 50 Å has been reported to be -0.5×10^{-6} emu g^{-1},[18] which is not so very different from that of ACF, despite the fact that the grain size of the fine-particles is larger than that of ACF. This means that in spite of the entangled appearance of ACF fibers, the micrographites of ACF are well graphitized compared with the grain of the graphite fine-particles. Here, we compare the estimated value of the orbital diamagnetic susceptibility with that of condensed aromatic hydrocarbons consisting of (N) benzene rings, in order to obtain information concerning the structure of the micrographitic domains. The relation between the number of benzene rings N and the value of $\chi_{//\text{orb}}$ for polycyclic aromatic compounds is shown in Fig. 6, after the data from the literature.[19] From a $\chi_{//\text{orb}}$ vs. N plot, we obtain an empirical relation expressed by

$$\log|\chi_{\text{orb}}| = -4.7 - 15\times\frac{1}{N}. \quad (5)$$

Using Eq. 5, the magnitude of $\chi_{//\text{orb}}$ for a condensed polycyclic aromatic compound with N=36, which is considered to correspond to the average structure of the micrographite in ACF, is expected to be -8.0×10^{-6} emu g^{-1}, which is about eight times larger than the experimental results for ACF1000 and ACF2000, as shown in Table 1. The cause of the difference between them is thought to be as follows. The deviation from the expected value of $\chi_{//\text{orb}}$ for model polycyclic aromatic compounds implies the presence of a distortion and/or

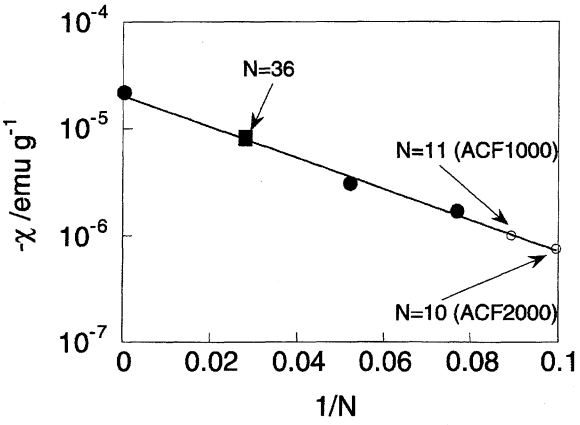

Fig. 6. The relation between the number of benzene rings N and the value of the orbital diamagnetic susceptibility χ_{orb} for condensed polycyclic aromatic compounds. ACF1000 (N=10) and ACF2000 (N=11) marked with ○ denote the positions corresponding to the experimentally obtained orbital susceptibility for ACF1000 and ACF2000, respectively, while ■ with N=36 corresponds to the number of benzene rings for the average structure of the micrographitic domain in ACF. The data for polycyclic compounds denoted by ● are referred from Ref. 20. N=11 and N=10 mean that the observed values of χ_{orb} correspond to the orbital susceptibilities of the compounds with 11 and 10 benzene rings for ACF1000 and 2000 respectively.

defects in the micrographite, which depresses the effective size of the π-electronic system in the micrographite. Again, by using Eq. 5, the number of benzene rings (N) which correspond to the observed value of $\chi_{//\text{orb}}$ is estimated to be N=12 and N=11 for the effective sizes of the π-electronic systems in ACF1000 and ACF2000, respectively. The magnitude of $\chi_{//\text{orb}}$ is correlated to the degree of delocalization of π-electrons in a graphite sheet, indicating the extent of the plane structure. Therefore, the experimental finding reveals that a graphene sheet of ACF is deformed with some degree of nonplanarity, caused by defects and distortions of the in-plane structure. An analogous observation has been reported for carbon ribbons. $\chi_{//\text{orb}}$ of a polyacrylonitrile-based carbon fiber (PAN-CF) and benzene-derived carbon fiber (BDF)[20] are explained by the folded ribbon model, which involves a micro-folded layer structure, proposed by McClure and Hickman.[21] Although ACF does not have any periodically folded graphene sheets like carbon ribbons, according to the present results, the micrographite in ACF has a nonplanar structure with defects, which look like craters on the moon's surface. We have two possible reasons why the micrographite has a nonplanar structure: One is that the degenerate π-electronic structure of graphite is solved due to the presence of defects; the other is that the presence of functional groups attached to the graphitic microdomains causes a steric hindrance, resulting in the generation of a nonplanarity in the graphitic microdomains.

Conclusions

The transport and magnetic properties of pitch-based

ACF1000 and ACF2000 with SSA≈1000 and 2000 $m^2 g^{-1}$ were investigated in order to obtain information concerning the micrographite network structure and internal structure of a micrographitic domain having a size of ca. 20 Å. The temperature dependencies of the conductivities for both ACF1000 and ACF2000 are described in terms of the two-dimensional variable-range hopping mechanism, the behaviors of which are extrapolated to the ordinary thermally activation hopping conduction with an activation energy (E_a) of 60—80 meV in the higher temperature range. The dimensionality of the transport properties of ACF is supposed to be caused by the specific network structure of the micrographitic domains, which are linked to each other through bridges comprising σ-bonding carbons. Assuming that the localization length can be regarded as being equal to the domain size, the densities of the states at the Fermi energy level are estimated at $N(E_F)\approx 10^{18}$ $eV^{-1} m^{-2}$ for both ACF1000 and ACF2000.

Introducing nitrogen gas or oxygen gas changes the electrical conductivity, which is caused by a change in the micrographite network structure. In addition to a structural modification due to the introduced gas, oxygen affects the electronic structure of ACF through the formation of weak chemical bonding between the dangling bonds and oxygen molecules.

The magnetic susceptibilities for both ACF1000 and ACF2000 show a Curie–Weiss temperature dependent susceptibility below 40 K, which suggests the presence of 10^{19} g^{-1} localized magnetic moments associated with the dangling bond spins attached to the peripheries of micrographite. The orbital diamagnetic susceptibilities ($\chi_{//orb}$) of ACF1000 and ACF2000 were estimated to be -1.2×10^{-7} and -1.1×10^{-7} emu g^{-1}, respectively, which are about one order of magnitude smaller than that expected for the condensed polycyclic aromatic hydrocarbons having the same number of benzene rings to the average number of benzene rings of ACF1000 and 2000. This proves that the graphene sheet of ACF is deformed with some degree of nonplanarity caused by defects and distortions of the in-plane structure.

Beneficial discussions with Professor Ko Sugihara, Professor Takuro Tsuzuku, and Dr. Keiko Matsubara are gratefully acknowledged. This work was supported by a Grant-in-Aid for Scientific Research No. 04242103 from the Ministry of Education, Science and Culture.

References

1) K. Kaneko, S. Ozeki, T. Suzuki, and K. Kakei, "Characterization of Porous Solid II," ed by F. Rodriguez-Reiniso et al., Elservier Science Publishers B. V., Amsterdam (1991), p. 429.
2) T. Suzuki and K. Kaneko, *Carbon*, **26**, 734 (1998).
3) A. M. Rao, A. W. P. Fung, M. S. Dresselhaus, and M. Endo, *J. Mater. Res.*, **7**, 1788 (1992).
4) M. Endo, K. Oshida, S. L. di Vittorio, M. S. Dresselhasus, and M. Shiraishi, "International Symp. on Fractal and Physically Adsorbed Molecular States," Chiba, Japan, May 14—15, 1992.
5) K. Kakei, C. Ishii, M. Ruike, H. Kuwabara, and K. Kaneko, *Carbon*, **130**, 1075 (1992).
6) K. Kuriyama, *Tanso*, **155**, 282 (1992) (in Japanese).
7) S. L. di Vittorio, M. S. Dresselhaus, M. Endo, J.-P. Issi, L. Piraux, and V. Bayot, *J. Mater. Res.*, **6**, 778 (1991).
8) T. Enoki, K. Inukai, K. Suzuki, M. Endo, and N. Shindo, private communication.
9) S. Mrozowski, *Phys. Rev.*, **85**, 609 (1952).
10) A. Nakayama, K. Suzuki, T. Enoki, S. L. di Vittorio, M. S. Dresselhaus, K. Koga, M. Endo, and N. Shindo, *Synth. Met.*, **55—57**, 3736 (1993).
11) A. Nakayama, K. Suzuki, T. Enoki, M. Endo, and N. Shindo, private communication.
12) N. Shindo, K. Tai, and Y. Matsumura, *Chem. Eng.*, **28**, 1 (1987).
13) N. Mott, in "Conduction in Non-Crystalline Material," Clarendon Press, Oxford (1987).
14) R. E. Frankline, *Proc. R. Soc. (London)*, **A209**, 196 (1951).
15) K. Kaneko, *Solid State Phys., (Japan)*, **27**, 403 (1992).
16) A. Nakayama, T. Enoki, K. Suzuki, C. Ishii, K. Kaneko, M. Endo, and N. Shindo, *Solid State Commun.*, **93**, 323 (1995).
17) D. B. Fishbach, *Phys. Rev.*, **123**, 1613 (1961).
18) D. E. Soule, C. W. Nezbeda, and A. W. Czanderna, *Rev. Sci. Instrum.*, **35**, 150 (1964).
19) R. McWeeny, *Proc. Phys. Soc.*, **A65**, 839 (1952).
20) K. Matsubara, K. Kawamura, and T. Tsuzuku, *Jpn. J. Appl. Phys.*, **25**, 1016 (1986).
21) J. W. McClure and B. B. Hickman, *Carbon*, **20**, 373 (1982).